Mössbauer and transport studies of amorphous and icosahedral Zr-Ni-Cu-Ag-Al alloys

Mössbauer and transport studies of amorphous and icosahedral Zr–Ni–Cu–Ag–Al alloys

Z M Stadnik[1,6]**, Ö Rapp**[2]**, V Srinivas**[2,3]**, J Saida**[4] **and A Inoue**[5]

[1] Department of Physics, University of Ottawa, Ottawa, Ontario, Canada K1N 6N5
[2] Solid State Physics, Kungliga Tekniska Högskolan 229, SE Stockholm 16440-Kista, Sweden
[3] Physics Department, Indian Institute of Technology, Kharagpur 721302, India
[4] Inoue Superliquid Glass Project, ERATO, Japan Science and Technology Corporation (JST), Sendai 982-0807, Japan
[5] Institute for Materials Research, Tohoku University, Sendai 980-8577, Japan

E-mail: stadnik@physics.uottawa.ca

Abstract

The alloy $Zr_{65}Al_{7.5}Ni_{10}Cu_{7.3}Fe_{0.2}Ag_{10}$ in the amorphous and icosahedral states, and the bulk amorphous alloy $Zr_{65}Al_{7.5}Ni_{10}Cu_{7.5}Ag_{10}$, have been studied with ^{57}Fe Mössbauer spectroscopy, electrical resistance and magnetoresistance techniques. The average quadrupole splitting in both alloys decreases with temperature as $T^{3/2}$. The average quadrupole splitting in the icosahedral alloy is the largest ever reported for a metallic system. The lattice vibrations of the Fe atoms in the amorphous and icosahedral alloys are well described by a simple Debye model, with the characteristic Mössbauer temperatures of 379(29) and 439(28) K, respectively. Amorphous alloys $Zr_{65}Al_{7.5}Ni_{10}Cu_{7.5}Ag_{10}$ and $Zr_{65}Al_{7.5}Ni_{10}Cu_{7.3}Fe_{0.2}Ag_{10}$ have been found to be superconducting with the transition temperature, T_c, of about 1.7 K. The magnitude of T_c and the critical field slope at T_c are in agreement with previous work on Zr-based amorphous superconductors, while the low-temperature normal state resistivity is larger than typical results for binary and ternary Zr-based alloys. The resistivity of icosahedral $Zr_{65}Al_{7.5}Ni_{10}Cu_{7.3}Fe_{0.2}Ag_{10}$ is larger than that for the amorphous ribbon of the same composition, as inferred both from direct measurements on the ribbons and from the observed magnetoresistance. However the icosahedral sample is non-superconducting in the measurement range down to 1.5 K. The results for the resistivity and the superconducting T_c both suggest a stronger electronic disorder in the icosahedral phase than in the amorphous phase.

[6] Author to whom any correspondence should be addressed.

1. Introduction

Icosahedral (i) alloys can be produced by various processes [1]. One of them is through crystallization of a corresponding amorphous (a) phase. This process was used to produce i alloys in a few systems: Pd–U–Si [2], Al–Mn–Si [3, 4], Al–Cu–V [4, 5], Ti–Zr–Ni [6] and Ti–Ni–Cu–Si [7]. The studies of these systems revealed the presence of unusual physical properties associated with the quasiperiodic structure of these i alloys [8]. More recently, i alloys have been discovered via crystallization of an a phase in several Zr-based systems: Zr–Pd [9, 10], Hf–Pd [11], Zr–Pd–M (M = Fe, Co, Ni, Cu) [10, 12, 13], Zr–M (M = Pt, Au)–Ni [13], Zr–Cu–Al [14, 15] and Zr–Cu–Ti–Ni [16].

Amorphous alloys (glasses) are generally produced from an undercooled liquid state by rapid quenching techniques or quasi-statically at slow cooling [17]. The latter technique has recently led to the development of multicomponent a alloys (bulk a alloys) with large glass forming ability and a wide supercooled liquid region before crystallization [18]. Very recently, i phases have been found via devitrification of such bulk a alloys in the quaternary Zr–Cu–Ni–Al [14, 19], Zr–M (M = Pd, Pt, Au)–Ni–Al [20] and Hf–Cu–Ni–Al [21] and penternary Zr–Cu–Ni–Al–M (M = Ti, V, Nb, Pd, Ag, Ta, Ir, Pt, Au) [22–34], Zr–Be–Ni–Ti–Cu [35] and Hf–Cu–Ni–Al–M (M = Ti, Pd) systems [34, 36, 37]. Surprisingly, no studies of the physical properties of these new Zr- and Hf-based i alloys have been reported.

In this paper, we report on the studies of a and i penternary alloys Zr–Al–Ni–Cu–Ag of the same composition with Mössbauer spectroscopy, electrical resistance and magnetoresistance techniques.

2. Experimental procedure

An alloy of nominal composition $Zr_{65}Ni_{10}Ag_{10}Cu_{7.3}Fe_{0.2}Al_{7.5}$ was prepared by arc melting in an argon atmosphere of high-purity elemental constituents; the Fe metal used was enriched to 95.9% in the ^{57}Fe isotope. The Fe atoms are believed to substitute on the Cu sites due to the closeness of the metallic radii of Cu (1.28 Å) and Fe (1.27 Å). Amorphous ribbons were prepared by melt spinning in an argon atmosphere. They were about 3 cm long, 1 mm wide and 20 μm thick. The differential scanning calorimetry (DSC) measurements at a heating rate of 0.67 K s^{-1} were performed to study the thermal behaviour of the alloy. An isothermal anneal of the a ribbons was carried out at 570 K for 15 min in a quartz tube evacuated to a vacuum of about 10^{-5} Torr. This resulted in the appearance of nanoscale spherical i precipitates. X-ray diffraction (XRD) was performed on the as-spun and annealed samples using Cu Kα radiation in the 2Θ–Θ configuration. The diffractometer was calibrated with Si (National Institute of Standards and Technology reference material 640c) as an internal standard. Transmission electron microscopy (TEM) was carried out on the specimens thinned by ion milling using a JEOL JEM-3000F microscope operated at 300 kV. A bulk a alloy of nominal composition $Zr_{65}Ni_{10}Ag_{10}Cu_{7.5}Al_{7.5}$ in the form of a cylinder with a diameter of 3 mm and length 4 mm was produced by copper mould casting [38].

^{57}Fe MS measurements were carried out in the temperature range 77–300 K using a standard Mössbauer spectrometer operating in a sine mode [39]. The spectrometer was calibrated with a 6.35 μm Fe foil, and the spectra were folded. The Mössbauer absorbers of the i and a alloys had the same surface density of 0.043 mg ^{57}Fe cm^{-2}. This corresponds to the effective thickness parameter [39] at 299 K of 0.852 and 0.920 (using the values of the absorber Debye–Waller factors, f_a and f_i, of 0.732 and 0.791 determined below), respectively. As the resulting Mössbauer spectra are due to multiple elementary quadrupole doublets, the effective thickness parameter spreads over them and therefore the absorbers can be regarded as being thin [39].
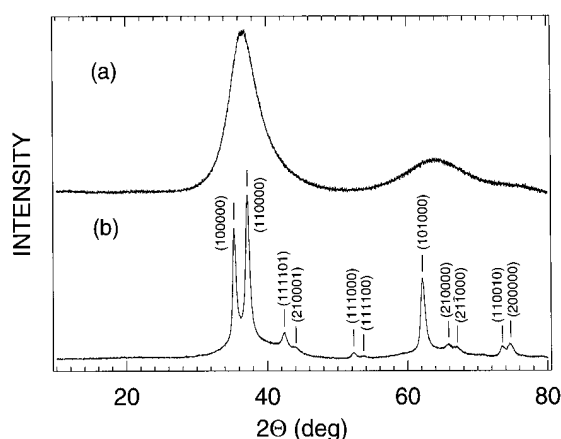
Figure 1. XRD patterns of (a) the melt-spun and (b) annealed $Zr_{65}Ni_{10}Ag_{10}Cu_{7.3}Fe_{0.2}Al_{7.5}$ alloy. The positions of the i peaks in (b), which are labelled using the indexing scheme of Bancel *et al* [40], are indicated with the vertical lines.

Electrical transport measurements were carried out with a conventional four-probe silver contact dc technique on amorphous and quasicrystalline ribbons with dimensions about $10 \times 1 \times 0.030$ mm^3 as well as on the bulk a cylinder of diameter of about 3 mm. The electrical resistance was measured in the temperature range 1.5–300 K. The magnetoresistance was studied in magnetic fields up to 12 T at temperatures in the range up to 12 K in a continuous gas flowing cryostat. Temperature drift during field sweeps was reduced to a few millikelvin using a regulated shielded vacuum space and a high-purity copper sample holder extending into a field-free region above the solenoid. Temperature errors during field scans were therefore negligible.

3. Results and discussion

3.1. Structural characterization

The XRD pattern of the melt-spun $Zr_{65}Ni_{10}Ag_{10}Cu_{7.3}Fe_{0.2}Al_{7.5}$ ribbon is characteristic of an a structure (figure 1(a)) with two broad peaks located at positions characterized by wavenumbers Q ($Q = 4\pi \sin \Theta / \lambda$, where 2Θ is the scattering angle and λ is the wavelength of the probing radiation) of 2.557(2) and 4.317(6) Å^{-1}. The same pattern was also observed for the bulk $Zr_{65}Ni_{10}Ag_{10}Cu_{7.5}Al_{7.5}$ alloy. The amorphous nature of these two specimens was also corroborated by TEM micrographs and electron diffraction patterns.

The DSC curve of a-$Zr_{65}Ni_{10}Ag_{10}Cu_{7.3}Fe_{0.2}Al_{7.5}$ shows (figure 2(a)) that the crystallization proceeds through two exothermic peaks. The onset crystallization temperatures of these peaks are, respectively, 705(1) and 770(1) K. The first peak results from the formation of an i phase and the second peak corresponds to the transformation of the i phase into a crystalline phase [28–30]. The DSC curve of the $Zr_{65}Ni_{10}Ag_{10}Cu_{7.3}Fe_{0.2}Al_{7.5}$ alloy isothermally annealed at 570 K for 15 min shows (figure 2(b)) that the first peak decreased dramatically, which indicates that the annealed sample consists mostly of the i phase.

The XRD pattern of the annealed $Zr_{65}Ni_{10}Ag_{10}Cu_{7.3}Fe_{0.2}Al_{7.5}$ (figure 1(b)) exhibits Bragg peaks which can be indexed to the i structure. The value of the six-dimensional hypercubic lattice constant calculated from the fitted position of the (100 000) peak [40] is 7.605(2) Å.
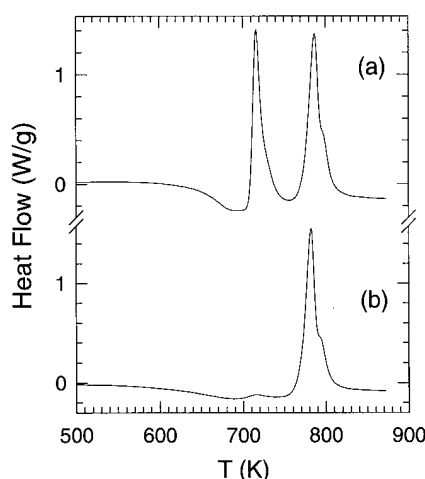
Figure 2. DSC scans of (a) melt-spun and (b) isothermally annealed $Zr_{65}Ni_{10}Ag_{10}Cu_{7.3}Fe_{0.2}Al_{7.5}$ alloy.

The two strongest i peaks are superimposed on a wide maximum located at $Q = 2.588(7)$ Å^{-1} (figure 1(b)) which is due to the presence of residual (relaxed) a phase in the annealed sample.

The bright-field TEM image of the annealed $Zr_{65}Ni_{10}Ag_{10}Cu_{7.3}Fe_{0.2}Al_{7.5}$ shows (figure 3(a)) that the i phase is in the form of nearly spherical particles, with an average diameter of about 30 nm, embedded in an a matrix. The nano-beam electron diffraction pattern of the annealed $Zr_{65}Ni_{10}Ag_{10}Cu_{7.3}Fe_{0.2}Al_{7.5}$ reveals (figures 3(b)–(d)) the fivefold, threefold and twofold symmetries compatible with the i structure. No diffraction spots originating from other crystalline phases could be observed in the nano-beam diffraction.

Mössbauer spectra of the amorphous and annealed $Zr_{65}Al_{7.5}Ni_{10}Cu_{7.3}Fe_{0.2}Ag_{10}$ (figure 4) measured in a wide velocity range show patterns due to the presence of only the electric quadrupole interaction; no patterns due to the presence of magnetically ordered Fe-containing second phases are detected.

The structural characterization described above shows that the a samples are in a pure amorphous state, whereas the annealed $Zr_{65}Al_{7.5}Ni_{10}Cu_{7.3}Fe_{0.2}Ag_{10}$, referred to later as the i alloy, consists largely of the i phase and a residue of the a phase.

3.2. Mössbauer spectroscopy

The Mössbauer spectrum of the a alloy consists of a broadened asymmetric doublet (figure 5(a)) which results from the distribution of the quadrupole splittings, $P(\Delta)$. It was fitted with the constrained version [41] of the Hesse–Rübartsch method. An asymmetry of the spectrum was accounted for by assuming a linear relation between the centre shift, δ, and Δ of the elementary Lorentzian doublets with width of 0.230 mm s^{-1}. A good fit, as judged by the value of $\chi^2 = 1.15$ and by the residuals (figure 5(a)), was obtained for the distribution $P(\Delta)$ shown in figure 5(c). It would be desirable to compare this distribution with the one calculated for a structural model of the Zr–Al–Ni–Cu–Ag glasses. Unfortunately, such a model has not been proposed yet for these new a alloys.

The Mössbauer spectrum of the i alloy (figure 5(b)) can be fitted with only two subspectra. The hyperfine parameters and the distribution $P(\Delta)$ of the first subspectrum (figure 5(c)) are very close to those corresponding to the a alloy. This is consistent with the fact that the i sample
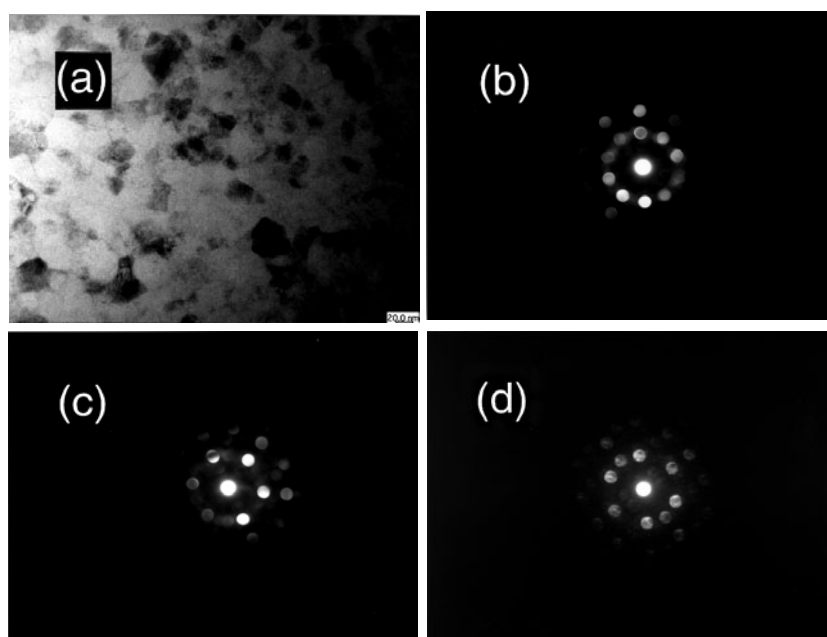
Figure 3. Bright-field TEM image (a) and nano-beam electron diffraction patterns corresponding to fivefold (b), threefold (c) and twofold (d) symmetries of the isothermally annealed $Zr_{65}Ni_{10}Ag_{10}Cu_{7.3}Fe_{0.2}Al_{7.5}$ alloy. The beam diameter for nano-beam electron diffraction is about 2.4 nm.
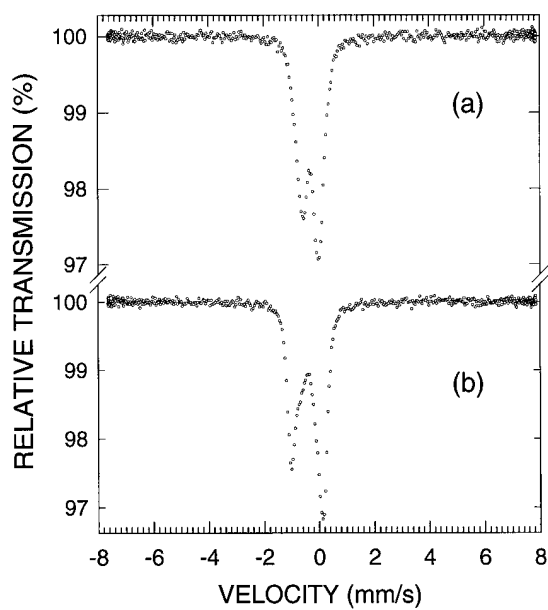

Figure 4. ^{57}Fe Mössbauer spectra at 299 K of (a) a and (b) i alloys $Zr_{65}Al_{7.5}Ni_{10}Cu_{7.3}Fe_{0.2}Ag_{10}$. The velocity scale is relative to α-Fe.
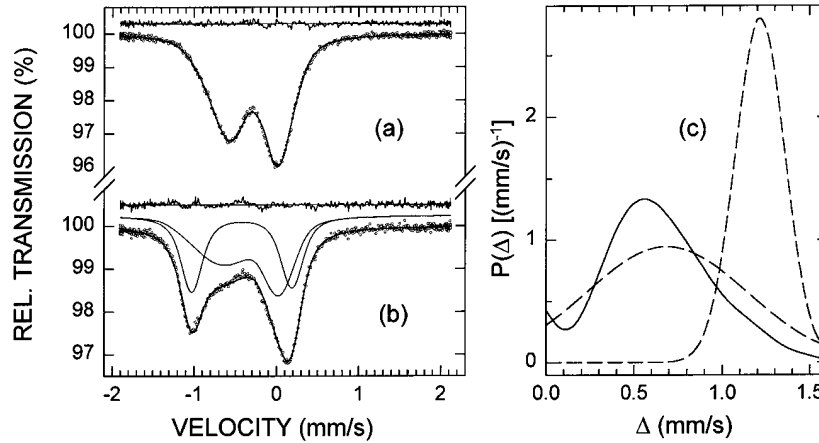
Figure 5. ^{57}Fe Mössbauer spectra at 299 K of (a) a and (b) i alloys $Zr_{65}Al_{7.5}Ni_{10}Cu_{7.3}Fe_{0.2}Ag_{10}$ fitted (solid curves in (a) and (b)), respectively, with one $P(\Delta)$ component (solid curve in (c)) and two $P(\Delta)$ components (dashed curves in (c)). The component fitted spectra are also shown in (b). The residuals are shown above each spectrum. The velocity scale is relative to α-Fe.

consists of nanoscale i clusters embedded in the a matrix. The weight fraction of the i phase calculated from the relative area of the subspectrum and the values of f_a and f_i is 41(4)%. The second subspectrum results from the i phase present in the i sample. Its remarkable feature is the very large value of the average quadrupole splitting, $\bar{\Delta}$, which is the largest ever observed for any quasicrystalline alloy [42] and, to the best of our knowledge, the largest ever found for any metallic alloy. Such a high value of $\bar{\Delta}$ indicates an unusually asymmetric atomic environment around the Cu atoms in the i phase.

Although there are no structural models for the a-Zr–Al–Ni–Cu–Ag alloys, it has been speculated [28, 31, 32] that the structure of these alloys is an assembly of randomly oriented i clusters, which presumably are also the structural units in i-Zr–Al–Ni–Cu–Ag alloys. The speculation that the a-Zr–Al–Ni–Cu–Ag alloys have a micro-quasicrystalline, rather than truly amorphous structure is based on the observation that the i phase precipitates directly from a-Zr–Al–Ni–Cu–Ag alloys [28, 31] and on a qualitative comparison between activation energies associated with transformation of the a phase into the i and crystalline phases [32]. The fact that the distribution $P(\Delta)$ corresponding to the i phase is completely different from that corresponding to the a phase (figure 5(c)) indicates that the structure of a-Zr–Al–Ni–Cu–Ag alloys cannot be described in terms of a micro-quasicrystalline model.

Distributions $P(\Delta)$ similar to those in figure 5(c) were determined from the fits of the a and i samples measured at other temperatures. The temperature dependence of $\bar{\Delta}$ could be fitted (figure 6) to the empirical equation

$$\bar{\Delta}(T) = \bar{\Delta}(0)(1 - BT^{3/2}), \qquad (1)$$

where $\bar{\Delta}(0)$ is the value of $\bar{\Delta}$ at 0 K and B is a constant. Such a $T^{3/2}$ temperature dependence has been observed in many metallic noncubic crystalline alloys [43], in some a alloys [44, 45], and recently in i alloys [45, 46] over temperature ranges from a few kelvins to the melting point. This seemingly universal $T^{3/2}$ dependence is not well understood. Its origin seems to be associated with a strong temperature dependence of mean-square lattice displacements and, to a lesser extent, with the temperature dependence of lattice expansion [47]. The values of $\bar{\Delta}(0)$ and B determined from the fits for the a and i phases are respectively 0.6847(20) mm s^{-1}, 1.489(88) $\times$ 10^{-5} K$^{-3/2}$ mm s^{-1} and 1.2610(29) mm s^{-1}, 1.122(69) $\times$ 10^{-5} K$^{-3/2}$ mm s^{-1}.
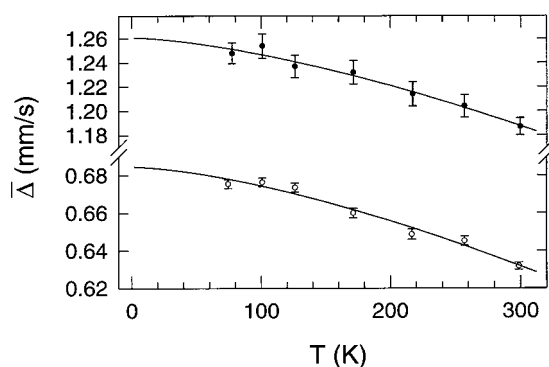
Figure 6. Temperature dependence of the average quadrupole splitting of the a (open circles) and i (closed circles) alloys $Zr_{65}Al_{7.5}Ni_{10}Cu_{7.3}Fe_{0.2}Ag_{10}$. The solid curves are the fits, as explained in the text.
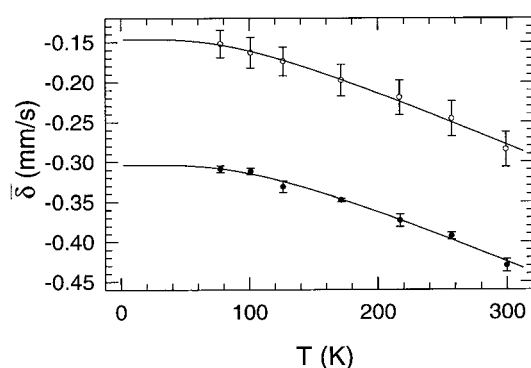

Figure 7. Temperature dependence of the average centre shift (relative to α-Fe) of the a (open circles) and i (closed circles) alloys. The solid curves are the fits, as explained in the text.

The average centre shift at temperature T, $\bar{\delta}(T)$, determined from the fits of the spectra of the a and i samples is given by

$$\bar{\delta}(T) = \delta_0 + \delta_{SOD}(T), \tag{2}$$

where δ_0 is the intrinsic isomer shift and $\delta_{SOD}(T)$ is the second-order Doppler (SOD) shift which depends on lattice vibrations of the Fe atoms [39]. In terms of the Debye approximation of the lattice vibrations, $\delta_{SOD}(T)$ is expressed [48] by the characteristic Mössbauer temperature Θ_M (Θ_M is distinct from the Debye temperature, Θ_D, determined from specific heat measurements, which is based on different weight of the phonon frequency distribution [47]) as

$$\delta_{SOD}(T) = -\frac{9}{2}\frac{k_B T}{Mc}\left(\frac{T}{\Theta_M}\right)^3 \int_0^{\Theta_M/T} \frac{x^3 \, \mathrm{d}x}{\mathrm{e}^x - 1}, \tag{3}$$

where M is the mass of the Mössbauer nucleus and c is the speed of light. By fitting the experimental data $\bar{\delta}(T)$ (figure 7) to equation (2), the quantities δ_0 and Θ_M can be determined. They are $-0.1464(35)$ mm s^{-1}, 379(29) K and $-0.3034(29)$ mm s^{-1}, 439(28) K, respectively, for the a and i samples.

The value of δ_0 depends on the s-electron density at the Mössbauer nucleus [39]. The significantly smaller value of δ_0 for the i alloy in comparison with the value for the a alloy

indicates that there is a much larger s-electron density in the former than in the latter alloy. This indicates that the electronic properties of the a and i alloys are very different.

Once Θ_M is known, the Debye–Waller factor at any temperature can be determined from

$$f(T) = \exp\left\{-\frac{3E_\gamma^2}{Mc^2 k_B \Theta_M}\left[1 + 4\left(\frac{T}{\Theta_M}\right)^2 \int_0^{\Theta_M/T}\frac{x\,\mathrm{d}x}{\mathrm{e}^x - 1}\right]\right\}, \tag{4}$$

where E_γ is the energy of the Mössbauer γ-ray transition. The values of f_a and f_i at 299 K calculated from equation (4) are, respectively, 0.732(36) and 0.791(24). This implies that on average the Fe atoms are more firmly bound in the i than in the a alloys.

3.3. Resistivity

Electrical transport properties of binary Zr-based a alloys have been extensively studied in the past. Some characteristic properties for Zr-rich a alloys are the following. These alloys are often superconducting with a transition temperature which is a remarkably simple function of the average electron number per atom [49]. The upper critical fields are frequently anomalously enhanced [50]. The temperature derivative of the electrical resistivity at room temperature is proportional to the electron–phonon coupling constant, λ [51]. Quantum interference effects have been convincingly demonstrated at low temperatures in non-superconducting a alloys [52]. Hence one expects these effects to be present also in amorphous superconductors of similar normal state resistivities, although this is more difficult to verify unambiguously due to the additional complication of the effects of superconducting fluctuations.

The temperature dependences of the electrical resistance of the a ribbon and bulk samples are shown in figure 8. Due to the uncertain geometrical form factor for the cylindrical sample, this comparison is best performed in terms of normalized resistance. It can be seen (figure 8) that the temperature coefficient of resistivity is negative in both cases, with average values as measured by the resistance ratio R ($=\rho(4\text{ K})/\rho(250\text{ K})$) of about 1.02 and 1.04 for the bulk and ribbon samples, respectively. Such values are typical for a alloys with resistivities in excess of about 150 $\mu\Omega$ cm.

Both the bulk and ribbon a samples are superconducting below about 1.7 K, with only small differences in T_c between the two samples. The magnitude of T_c is in agreement with that expected from the relation between T_c and average group number for Zr-based amorphous alloys [49] (counting 11 for Cu, as customary, and three for Al). The small replacement of 0.2 at.% Cu by Fe in the ribbon sample has a negligible effect on this scale. However, the transition width of about 0.8 K for the bulk a sample is considerably larger than the width of below 0.2 K for the ribbon sample. This is probably due to disorder associated with larger compositional fluctuations in the larger and more slowly cooled bulk sample.

Figure 9 shows the temperature variation of the resistivity, ρ, for the a and quasicrystalline ribbons down to 1.5 K. ρ is about 280 $\mu\Omega$ cm at 4 K for the a ribbon, which is significantly larger than the results around 180 $\mu\Omega$ cm for Zr-based alloys based on two or three elements. Although the structure for the present sample is not known, we can speculate that the short-range order in a six-component alloy is less well defined, and leads to larger compositional fluctuations and an enhanced resistivity.

ρ of the i alloy is larger than that of the a alloy. Although measurements on melt-spun ribbons tend to overestimate the resistivity due to the surface roughness of melt-spun samples, this error can be expected to have the same sign for both samples in figure 9. Therefore the observed difference between the samples is probably significant. This is also supported by the results for the magnetoresistance to be described below. A larger resistivity for the i sample is in agreement with the well known result that quasicrystalline order in stable quasicrystals
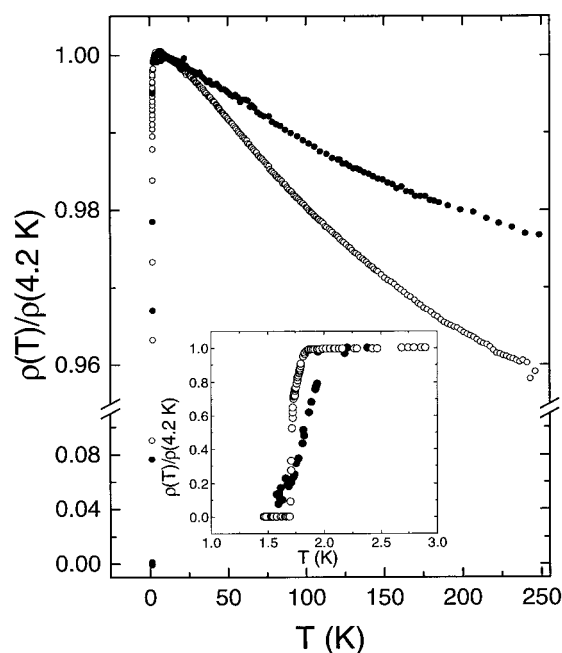
Figure 8.   Normalized resistivity as a function of temperature for bulk a alloy $Zr_{65}Al_{7.5}Ni_{10}Cu_{7.5}Ag_{10}$ (closed circles) and ribbon a alloy $Zr_{65}Al_{7.5}Ni_{10}Cu_{7.3}Fe_{0.2}Ag_{10}$ (open circles). Inset: enlargement in the region of the superconducting transition temperature.

gives larger resistivities than for a samples of similar chemical composition [8]. However, in a recent investigation of a and i phases of samples of the same nominal composition as the present Zr–Al–Ni–Cu–Ag samples, it was found in contrast that ρ at 300 K was insignificantly larger ($\approx 1\%$) for the i phase than for the a phase [53].

The low-temperature resistivity is shown in the inset of figure 9. The i sample is not superconducting in the measurement range down to 1.5 K, nor is there any sign of superconducting fluctuations. Thus if the i phase is superconducing one expects its T_c to be well below 1 K. Since the structural investigations indicate that the i phase is embedded in an a matrix of more than 50% of the sample volume, an a phase probably forms a percolating network through the i phase. The absence of superconductivity above 1.5 K in this sample therefore suggests that a proximity effect from the normal i phase depresses T_c of the a phase. This seems to be consistent with the structural investigations and the estimates of the coherence length, ξ, of several Zr-based a superconducors of about 5–7 nm [54]. A suppression of T_c would then result from a constriction in the percolating paths of the a phase of dimensions below about 10–15 nm.

It can be noted that in $Mg_3Zn_3Al_2$ the superconducting T_c is about three times larger for the a phase than for the i phase [55]. In this case the resistivity of the a phase is also larger than in the i phase, in similarity to most observations for i samples at that time, and the larger T_c of the a phase was ascribed to increased disorder. It is now realized that increased electronic disorder, as reflected for example in the large resistivities, and in the significant contributions of quantum corrections to electronic transport, is characteristic for a large number of stable i phases [8]. Furthermore, when band structure effects, for example from (further) smearing of the density of states, are negligible, T_c is always reduced by disorder [56]. For the present
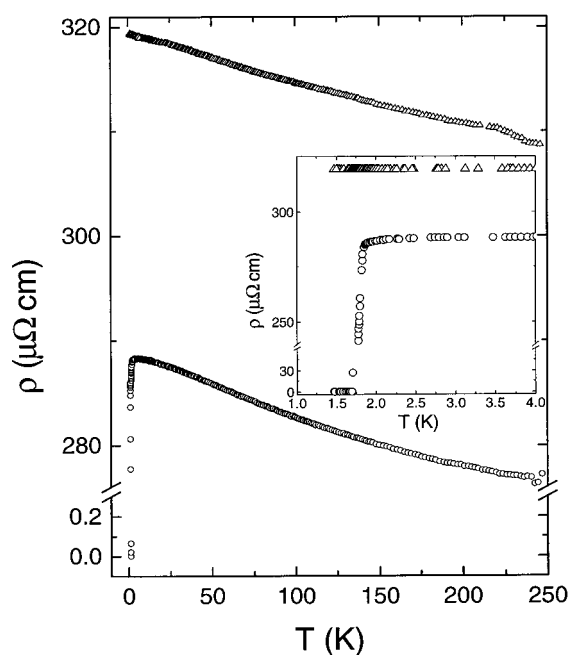
Figure 9. Resistivity as a function of temperature for a (open circles) and i (open triangles) $Zr_{65}Al_{7.5}Ni_{10}Cu_{7.3}Fe_{0.2}Ag_{10}$ ribbons. Inset: enlargement in the region of the superconducting transition temperature.

alloys the larger ρ and the smaller T_c of the i phase sample are thus both consistent with a larger electronic disorder in the i phase as compared with the a phase.

3.4. Magnetoresistivity

The magnetoresistances for the i and a phases are compared in figure 10 as a function of temperature at 12 T, and in figures 11(a) and (b) at several constant temperatures as a function of magnetic field. It was noted previously that the maximum observed magnetoresistance, $|\Delta\rho/\rho|$, is a universal function of the resistivity ρ at 4 K, and roughly follows $|\Delta\rho/\rho| \sim \rho^{1.3}$ over several orders of magnitude in ρ and for different non-superconducting materials, such as fcc alloys, a metals, decagonal and i quasicrystals and approximants [57]. From figure 11(a) the maximum $\Delta\rho/\rho$ for the i sample is of order 1.3×10^{-3}, which, according to the relation in [57], is characteristic for material with ρ (4 K) in the range of 400 ($\pm$25)% $\mu\Omega$ cm. Such a result is in fair agreement with ρ (4 K) for the i sample in figure 9, and supports our estimate for the resistivity of the i phase.

For the a sample, on the other hand, $\Delta\rho/\rho$ at 12 T and 3 K is three times larger than for the i sample (figure 10), in spite of the fact that the resistivity is smaller. This indicates that in addition to quantum interference effects there are further contributions to $\Delta\rho/\rho$ due to superconducting fluctuations. The temperature dependence of $\Delta\rho/\rho$ in figure 10, where $\Delta\rho/\rho$ falls off much faster with increasing temperature for the a sample, supports this interpretation. At 12 K, i.e. at $\sim 7T_c$, superconducting fluctuations are probably mostly quenched, and $\Delta\rho/\rho$ for the a sample is smaller than for the i sample as expected from the different resistivities. Unfortunately quantitative comparisons of quantum interference theories
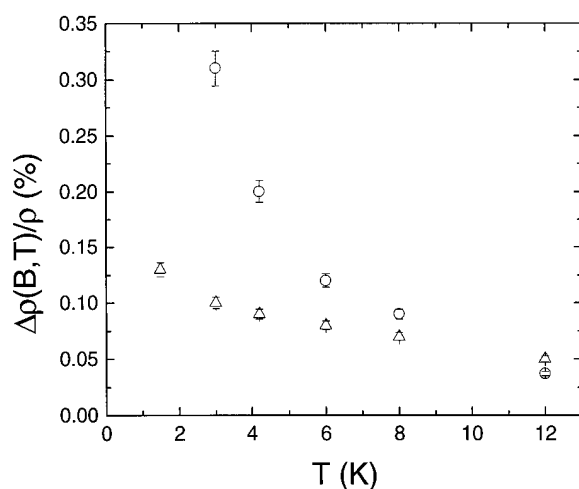
Figure 10. Temperature dependence of the magnetoresistance (at 12 T) for i-(open triangles) and a-(open circles) $Zr_{65}Al_{7.5}Ni_{10}Cu_{7.3}Fe_{0.2}Ag_{10}$ ribbons.
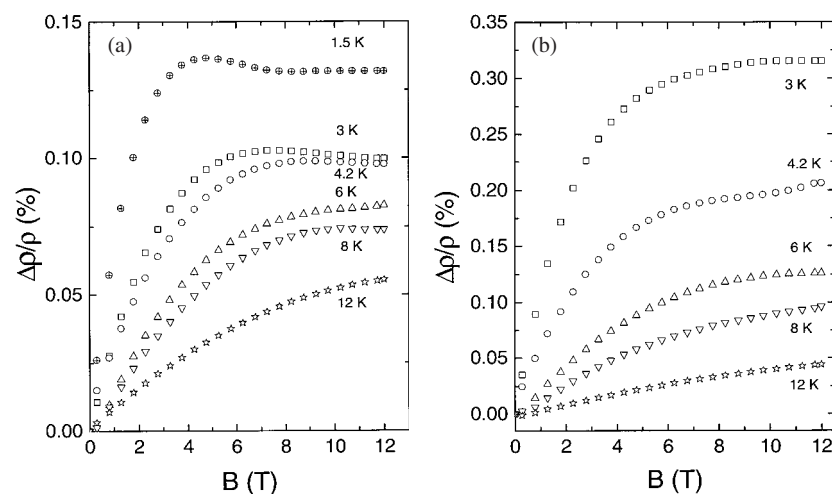

Figure 11. The magnetoresistance versus B for (a) i-and (b) a-$Zr_{65}Al_{7.5}Ni_{10}Cu_{7.3}Fe_{0.2}Ag_{10}$ ribbons taken at different temperatures.

for the magnetoresistance of a and i samples do not seem feasible due mainly to the difficulties of handling the fluctuation contributions in the experimental magnetic fields [58].

A few measurements were made on the superconducting samples in a magnetic field in the region of the transition. Although the temperature region available for these measurements, from 1.7 to 1.5 K, is limited, it can nevertheless be concluded that the midpoints of the resistive transitions were similarly depressed for the bulk and ribbon samples, with values of $-[dH_{c2}/dT]_{T_c}$ for both samples of roughly ~ 3 K T^{-1}. This result is of comparable magnitude to previous observations for a number of Zr-based superconductors with $-[dH_{c2}/dT]_{T_c}$ ranging from 2.8 to 3.6 K T^{-1} [54].

4. Conclusions

The average quadrupole splitting in both alloys decreases with temperature as $T^{3/2}$. The average quadrupole splitting in the icosahedral alloy is the largest ever reported for a metallic system. The lattice vibrations of the Fe atoms in the amorphous and icosahedral alloys are well described by a simple Debye model, with the characteristic Mössbauer temperatures of 379(29) and 439(28) K, respectively. Amorphous $Zr_{65}Al_{7.5}Ni_{10}Cu_{7.5}Ag_{10}$ with and without 0.2 at.% Fe substitution has been found to be superconducting with a T_c of about 1.7 K. The magnitude of T_c and the critical field slope at T_c are in agreement with previous work on Zr-based a superconductors, while the low-temperature normal state resistivity is larger than typical results for binary and ternary Zr-based alloys. The resistivity of i $Zr_{65}Al_{7.5}Ni_{10}Cu_{7.3}Fe_{0.2}Ag_{10}$ is larger than for the a ribbon of the same composition, as inferred both from direct measurements on the ribbons and from the observed magnitude of the magnetoresistance. The i sample was found to be non-superconducting in the measurement range down to 1.5 K. These results thus indicate a depression of superconductivity of the quasicrystal due to (electronic) disorder.

Acknowledgments

References

[1] Tsai A-P 1999 *Physical Properties of Quasicrystals* ed Z M Stadnik (Berlin: Springer) p 5
[2] Poon S J, Drehman A J and Lawless K R 1985 *Phys. Rev. Lett.* **55** 2324
   Shen Y, Poon S J and Shiflet G J 1986 *Phys. Rev.* B **34** 3516
   Drehman A J, Pelton A R and Noack M A 1986 *J. Mater. Res.* **1** 741
   Wong K M and Poon S J 1986 *Phys. Rev.* B **34** 7371
   Freeman J J, Dahlhauser K J, Anderson A C and Poon S J 1987 *Phys. Rev.* B **35** 2451
   Bretscher H, Grütter P, Indlekofer G, Jenny H, Lapka R, Oelhafen P, Wiesendanger R, Zingg T and
      Güntherodt H-J 1987 *Z. Phys.* B **68** 313
   Antonione C, Battezzati L, Marino F, Marazza R and Mazzone D 1989 *J. Less-Common Met.* **154** 169
[3] Inoue A, Bizen Y and Masumoto T 1988 *Metall. Trans.* A **19** 383
[4] Tsai A P, Inoue A, Bizen Y and Masumoto T 1989 *Acta Metall.* **37** 1443
   Tsai A P, Hiraga K, Inoue A, Masumoto T and Chen H S 1994 *Phys. Rev.* B **49** 3569
   Tsai A P, Inoue A and Masumoto T 1994 *Mater. Sci. Forum* **150/151** 275
   Tsai A P, Hiraga K, Inoue A, Masumoto T, Satoh K, Tsuda K and Tanaka M 1994 *Mater. Sci. Eng.* A **181–182**
      750
[5] Tsai A-P, Inoue A and Masumoto T 1987 *Japan. J. Appl. Phys.* **26** L1994
   Garçon S, Sainfort P, Regazzoni G and Dubois J M 1987 *Scr. Metall.* **21** 1493
   Matsubara E, Waseda Y, Tsai A P, Inoue A and Masumoto T 1988 *Z. Naturf.* a **43** 505
   Holzer J C and Kelton K F 1991 *Acta Metall. Mater.* **39** 1833
[6] Sibirtsev S A, Chebotnikov V N, Molokanov V V and Kovneristyi Yu K 1988 *JETP Lett.* **47** 744
   Molokanov V V and Chebotnikov V N 1990 *J. Non-Cryst. Solids* **117–118** 789
   Chebotnikov V N, Molokanov V V and Kovneristiy Yu K 1993 *Phase Transitions* **44** 215
   Murty B S, Kim W T, Kim D H and Hono K 2001 *Mater. Trans. JIM* **42** 372
[7] Alisova S P, Kovneristyi Yu K, Lazareva Yu E and Budberg P B 1990 *Dokl. Akad. Nauk SSSR* **315** 116
[8] Stadnik Z M (ed) 1999 *Physical Properties of Quasicrystals* (Berlin: Springer)
[9] Saida J, Matsushita M and Inoue A 2000 *J. Appl. Phys.* **88** 6081
   Murty B S, Ping D H and Hono K 2000 *Appl. Phys. Lett.* **77** 1102
   Saida J, Matsushita M, Li C and Inoue A 2001 *Phil. Mag. Lett.* **81** 39
[10] Zhang T, Inoue A, Matsushita M and Saida J 2001 *J. Mater. Res.* **16** 20
   Saida J, Matsushita M and Inoue A 2001 *Appl. Phys. Lett.* **79** 412
   Saida J, Matsushita M and Inoue A 2001 *J. Appl. Phys.* **90** 4717

Imafuku M, Saida J and Inoue A 2001 *J. Mater. Res.* **16** 3046

Jiang J Z, Saksi K, Saida J, Inoue A, Franz H, Messel K and Lathe C 2002 *Appl. Phys. Lett.* **80** 781

[11] Li C and Inoue A 2001 *Mater. Trans. JIM* **42** 176

[12] Matsushita M, Saida J, Li C and Inoue A 2000 *J. Mater. Res.* **15** 1280

Saida J, Matsushita M and Inoue A 2000 *Mater. Trans. JIM* **41** 543

[13] Saida J, Matsushita M, Li C and Inoue A 2000 *Appl. Phys. Lett.* **77** 3558

[14] Köster U, Meinhardt J, Ross S and Rüdiger A 1996 *Mater. Sci. Forum* **225–227** 311

[15] Murty B S, Ping D H, Hono K and Inoue A 2000 *Appl. Phys. Lett.* **76** 55

Murty B S, Ping D H, Hono K and Inoue A 2000 *Acta Mater.* **48** 3985

[16] Louzguine D V and Inoue A 2001 *Appl. Phys. Lett.* **78** 1841

[17] Greer A L 1995 *Science* **267** 1947

[18] Inoue A 2000 *Acta Mater.* **48** 279

[19] Köster U, Meinhardt J, Ross S and Liebertz H 1996 *Appl. Phys. Lett.* **69** 179

Köster U, Meinhardt J, Ross S and Busch R 1997 *Mater. Sci. Eng.* A **226–228** 995

Eckert J, Mattern N, Zinkevitch M and Seidel M 1998 *Mater. Trans. JIM* **39** 623

[20] Inoue A, Saida J, Matsushita M and Sakurai T 2000 *Mater. Trans. JIM* **41** 362

[21] Li C and Inoue A 2001 *J. Mater. Res.* **16** 1190

[22] Xing L Q, Eckert J, Löser W and Schultz L 1999 *Appl. Phys. Lett.* **74** 664

[23] Saida J and Inoue A 2001 *J. Phys.: Condens. Matter* **13** L73

[24] Saida J, Matsushita M, Li C and Inoue A 2000 *Phil. Mag. Lett.* **80** 737

Lee J K, Choi G, Kim W T and Kim D H 2001 *J. Mater. Res.* **16** 1311

Jiang J Z, Saksi K, Rasmussen H, Watanuki T, Ishimatsu N and Shimomara O 2001 *Appl. Phys. Lett.* **79** 1112

Han T K, Zhang T, Inoue A, Yang Y S, Kim I B and Kim Y H 2001 *Mater. Sci. Eng.* A **304–306** 892

Jiang J Z, Rasmussen A R, Jensen C H, Lin Y and Hansen P L 2002 *Appl. Phys. Lett.* **80** 2090

[25] Saida J, Matsushita M and Inoue A 2000 *Mater. Trans. JIM* **41** 1505

[26] Inoue A, Zhang T, Saida J and Matsushita M 2000 *Mater. Trans. JIM* **41** 1511

[27] Inoue A, Zhang T, Chen M W, Sakurai T, Saida J and Matsushita M 2000 *Appl. Phys. Lett.* **76** 967

[28] Chen M W, Zhang T, Inoue A, Sakai A and Sakurai T 1999 *Appl. Phys. Lett.* **75** 1697

[29] Saida J, Matsushita M, Zhang T, Inoue A, Chen M W and Sakurai T 1999 *Appl. Phys. Lett.* **75** 3497

[30] Matsushita M, Saida J, Zhang T, Inoue A, Cheng M W and Sakurai T 2000 *Phil. Mag. Lett.* **80** 79

[31] Chen M W, Inoue A, Zhang T, Sakai A and Sakurai T 2000 *Phil. Mag. Lett.* **80** 263

[32] Chen M W, Dutta I, Zhang T, Inoue A and Sakurai T 2001 *Appl. Phys. Lett.* **79** 42

[33] Li C and Inoue A 2001 *Phys. Rev.* B **63** 172201

[34] Murty B S, Ping D H, Hono K and Inoue A 2000 *Scr. Mater.* **43** 103

Saida J, Li C, Matsushita M and Inoue A 2001 *J. Mater. Res.* **16** 3389

[35] Wanderka N, Macht M-P, Seidel M, Mechler S, Stahl K and Jiang J Z 2000 *Appl. Phys. Lett.* **77** 3935

[36] Li C, Saida J, Matsushita M and Inoue A 2000 *Phil. Mag. Lett.* **80** 621

[37] Li C, Saida J, Matsushita M and Inoue A 2000 *Appl. Phys. Lett.* **77** 528

[38] Inoue A, Zhang T and Kim Y H 1997 *Mater. Trans. JIM* **38** 749

[39] Greenwood N N and Gibb T C 1971 *Mössbauer Spectroscopy* (London: Chapman and Hall)

[40] Bancel P A, Heiney P A, Stephens P W, Goldman A I and Horn P M 1985 *Phys. Rev. Lett.* **43** 2422

[41] Le Caër G and Dubois J M 1979 *J. Phys. E: Sci. Instrum.* **12** 1083

[42] Stadnik Z M 1996 *Mössbauer Spectroscopy Applied to Magnetism and Materials Science* vol 2, ed G J Long and F Grandjean (New York: Plenum) p 125

[43] Kaufmann E N and Vianden R J 1979 *Rev. Mod. Phys.* **51** 161 and references therein

[44] Deppe P and Rosenberg M 1983 *Hyperfine Interact.* **15–16** 735

Kopcewicz M, Kopcewicz B and Gonser U 1987 *J. Magn. Magn. Mater.* **66** 79

Mao M, Ryan D H and Altounian Z 1994 *Hyperfine Interact.* **92** 2163

[45] Stadnik Z M, Takeuchi T and Mizutani U 2000 *Mater. Sci. Eng.* A **294–296** 331

[46] Brand R A, Voss J and Calvayrac Y 2000 *Mater Sci. Eng.* A **294–296** 666

[47] Nishiyama K, Dimmling F, Kornrumph Th and Riegel D 1976 *Phys. Rev. Lett.* **37** 357

Jena P 1976 *Phys. Rev. Lett.* **36** 418

Christiansen J, Heubes P, Keitel R, Klinger W, Loeffler W, Sandner W and Witthuhn W 1976 *Z. Phys.* B **24** 177

[48] Kolk B 1984 *Dynamical Properties of Solids* vol 5, ed G K Horton and A A Maradudin (Amsterdam: North-Holland) p 3

[49] Poon S J and Carter W L 1980 *Solid State Commun.* **35** 249

[50] Poon S J 1983 *Amorphous Metallic Alloys* ed F E Luborsky (London: Butterworths) p 432

[51] Rapp Ö, Jäckle J and Froböse K 1981 *J. Phys. F: Met. Phys.* **11** 2359

[52] Lee P A and Ramakrishnan T V 1985 *Rev. Mod. Phys.* **57** 287
[53] Haruyama O, Miyazawa T, Saida J and Inoue A 2001 *Appl. Phys. Lett.* **79** 758
[54] Karkut M G and Hake R R 1983 *Phys. Rev.* B **28** 1396
[55] Graebner J E and Chen H S 1987 *Phys. Rev. Lett.* **58** 1945
[56] Belitz D and Kirkpatrick T R 1994 *Rev. Mod. Phys.* **66** 261
[57] Rapp Ö 1999 *Physical Properties of Quasicrystals* ed Z M Stadnik (Berlin: Springer) p 126
[58] Larkin A I 1980 *Pis. Eksp. Teor. Fiz.* **31** 239 (Engl. transl. 1980 *JETP Lett.* **31** 219)
     McLean W L and Tsuzuki T 1984 *Phys. Rev.* B **29** 503
     Lopez dos Santos J M B and Abrahams E 1985 *Phys. Rev.* B **31** 172